

Response to Reviewers

Reviewer comments are in black.

Author responses are in blue.

Changes made to the manuscript are in red.

Reviewer #1 (RC1)

Review Summary

The manuscript presents an open-access Lagrangian air-parcel trajectory dataset spanning 1979 to 2024, generated using FLEXPART v11 and ERA5 reanalysis data. The authors provide a valuable Lagrangian climatology to the research community, intended for studying moisture and heat transport. Additionally, the paper introduces version 2 of the Heat And Moisture Tracking framEwoRk (HAMSTER) for post-processing and provides illustrative examples of the dataset's applications. While the paper is well-written and the dataset has clear value, several key concerns regarding novelty and methodological justification should be addressed before it can be considered for publication.

Specific Comments

1. The manuscript would benefit from a more thorough comparison with existing literature. The proposed dataset is not unique; at least two similar datasets cover comparable periods: the LARA dataset (Bakels et al., 2025) and the dataset provided by Vázquez et al. (2024) (using FLEXPART v10.3 and ERA5). The authors must explicitly discuss how this new global dataset improves upon or complements these existing records to justify its publication.

Author response: We thank the reviewer for this important comment. We agree that several recent efforts have produced global Lagrangian trajectory datasets, including LARA (Bakels et al., 2025) and the FLEXPART-ERA5 simulations by Vázquez et al. (2024). We have revised the manuscript to more clearly position our dataset in relation to these existing resources.

While the general concept of domain-filling Lagrangian simulations is shared, our dataset differs in several aspects and is intended to complement, rather than replace, these existing datasets.

First, compared to Vázquez et al. (2024), our simulations are based on FLEXPART v11, which includes several changes e.g. improvement in wet deposition, cloud identification, precipitation interpolation, and trajectory accuracy through better particle density distribution. In addition, our dataset is fully open access and readily usable without the requirement for individual data requests.

Second, compared to LARA, our simulations use a substantially higher number of particles (~20 million versus 6 million), which increases the sampling density of the atmosphere and improves the robustness of statistical analyses, especially at regional scales (see next comment). Additionally, LARA is designed as a continuous Lagrangian reanalysis with multi-year particle integration, whereas our dataset follows a year-by-year simulation strategy with consistent particle initialization. This design limits the accumulation of trajectory errors associated with very long continuous integrations, and facilitates the construction of temporally consistent climatologies, which is particularly advantageous for hydroclimatic and source–receptor analyses.

Overall, we view the dataset presented here as complementary to existing Lagrangian trajectory archives, providing an alternative configuration that is particularly suited for hydroclimatic applications, including trend analysis (due to the annual reinitialisation) and extreme events (given the high number of parcels), and that can be easily integrated with diagnostic frameworks such as HAMSTER. Additionally, the availability of multiple global Lagrangian datasets enables intercomparison studies to assess the impact of methodological choices, such as particle number and simulation configuration.

Changes: We replaced the last paragraph of the introduction by the following two paragraphs (L102–114):

“Here we present a global Lagrangian trajectory dataset covering the period 1979–2024. By providing the full trajectory archive directly, the dataset enables efficient analysis of atmospheric moisture and heat pathways without the need to rerun computationally expensive simulations. The dataset builds on recent efforts to produce global Lagrangian trajectory archives based on FLEXPART and ERA5 (e.g., Bakels et al., 2025; Vázquez et al., 2025). While these datasets share a similar modelling approach, the dataset presented here adopts a complementary configuration. Compared to Vázquez et al. (2025), our simulations use FLEXPART v11, which includes improvements in trajectory accuracy and process representation, and are fully open-access. Compared to LARA (Bakels et al., 2025), which provides continuous multi-year trajectories, our dataset follows a year-by-year simulation strategy with consistent particle initialization, limiting error accumulation and facilitating temporally consistent climatologies and trend analysis. In addition, the higher number of particles improves atmospheric sampling, particularly for regional analyses and studies of hydrometeorological extremes. Overall, this dataset complements existing trajectory archives and is particularly suited for hydroclimatic applications and integration with diagnostic frameworks such as HAMSTER. We demonstrate the dataset’s applicability using global climatologies and event-scale case studies, and provide the full trajectory archive together with the HAMSTER v2 post-processing tool as open-access resources.”

2. The authors utilised a domain-filling mode with 20 million air parcels. A more robust justification for this specific configuration is required. Specifically, were sensitivity tests performed to determine the optimal number of parcels? A brief discussion on how the

parcel count impacts the reliability and statistical significance of the results would provide greater confidence in the dataset.

Author response: The choice of 20 million particles was guided by both sensitivity experiments and theoretical considerations of Lagrangian sampling in FLEXPART.

We performed a series of sensitivity tests using an earlier FLEXPART (v10.4) and HAMSTER (v1) configuration, in which both the number of vertical levels (45, 60, 75, 90, and 137 levels) and the particle count were varied. These experiments showed that increasing the vertical resolution beyond ~90 levels resulted in only marginal improvements in the diagnosed evaporation, precipitation, and sensible heat flux fields, while substantially increasing computational cost (Figure 1). Similarly, increasing the number of particles beyond approximately 10 million produced only limited improvements in the large-scale diagnosed signals and spatial performance metrics (RMSE, MBE, and correlation), indicating convergence of the statistics (Figure 1 and 2).

In FLEXPART's domain-filling configuration, particles are distributed proportionally to atmospheric column mass. To evaluate whether the vertical structure is sufficiently sampled, FLEXPART internally defines the ratio

$$f = \frac{\max(n_{column})}{n_z} \text{ with } n_{column} \propto N_{particles} \cdot \frac{colmass}{colmass_{total}}$$

where n_z is the number of vertical levels. A value of $f < 1$ indicates insufficient sampling of the vertical structure (i.e. fewer than one particle per level even in the best-sampled column), and the model explicitly recommends increasing the number of particles in that case.

In our configuration:

- Total particles: 20 million
- Vertical levels: $n_z=91$
- Maximum particles per column: 129 (every yearly simulation is around this number)

This yields: $f \approx 1.41$

Although the sensitivity experiments suggested that 9 to 10 million particles already produced relatively stable large-scale statistics, the final choice of 20 million particles was made to satisfy the FLEXPART consistency criterion, improve sampling for regional and extreme-event analyses, and take advantage of the reduced computational cost and output size of the newer FLEXPART version used for the final simulations.

At 20 million particles, the sampling density is therefore sufficient to:

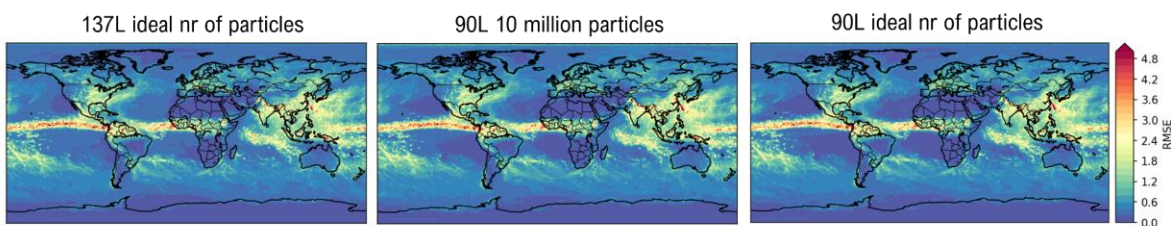
- Resolve vertical structure (as shown above).
- Ensure stable large-scale moisture fluxes.
- Provide robust statistics for climatological analyses.

- Maintain sufficient parcel sampling for regional and extreme-event analyses, where only a small fraction of global parcels contributes to the diagnosed sinks.

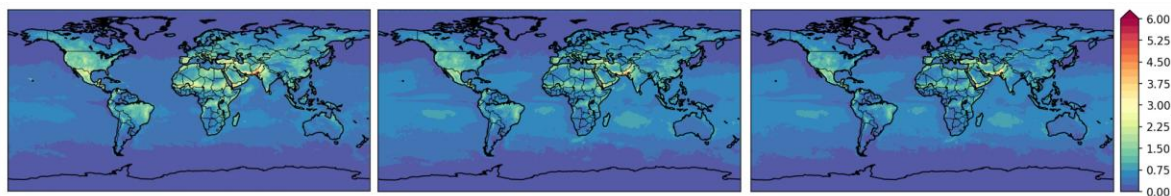
For comparison, lower particle counts—as used in other global trajectory datasets (e.g., ~6 million particles in LARA; see previous comment)—result in lower sampling densities and may fall below this internal consistency threshold, particularly when using a similar (or even higher) number of vertical levels.

We do not include the full sensitivity analysis in the manuscript because these experiments were performed with an earlier FLEXPART/HAMSTER setup (v10.4/v1), whereas the final dataset was generated using FLEXPART v11 and HAMSTER v2. As the sensitivity tests are therefore not fully consistent with the final production configuration, we consider them supportive rather than part of the core dataset evaluation.

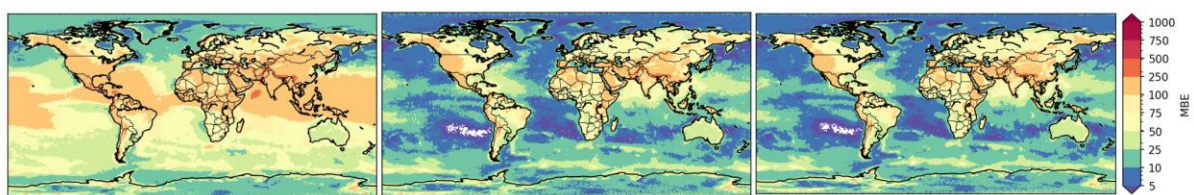
TEMPORAL PRECIPITATION



TEMPORAL EVAPORATION



TEMPORAL SSHF



Partposit every: ~33 min
Size 1 file: 2 078 149 KB

Partposit every: ~15 min
Size 1 file: 585 565 KB

Partposit every: ~17 min
Size 1 file: 1 365 890 KB

Figure 1: RMSE between ERA5 and the diagnosed precipitation, evaporation, and surface sensible heat flux fields obtained with FLEXPART v10.4 and HAMSTER v1 for different FLEXPART configurations: (i) 137 vertical levels with 35,609,040 particles (corresponding to the “ideal” particle count, defined as $137 \times 361 \times 720$); (ii) 90 vertical levels with 10 million particles; and (iii) 90 vertical levels with 23,392,800 particles (corresponding to $90 \times 361 \times 720$).

P	r	MBE	RMSE
45l 9 million	0.81	113.87	242.01
60l 9 million	0.81	88.44	207.26
60l ideal nr	0.83	24.75	103.07
75l 9 million	0.86	-21.94	87.10
75l ideal nr	0.87	-22.00	87.59
90l 10 million	0.93	-16.33	64.97
90l ideal nr	0.93	-16.15	65.02
137l ideal nr	0.92	1.18	65.82
E	r	MBE	RMSE
45l 9 million	0.32	145.93	335.00
60l 9 million	0.30	161.83	381.06
60l ideal nr	0.31	54.11	220.21
75l 9 million	0.36	0.71	157.36
75l ideal nr	0.37	1.96	155.69
90l 10 million	0.24	-47.81	154.52
90l ideal nr	0.24	-48.67	154.36
137l ideal nr	0.58	43.75	143.46
H	r	MBE	RMSE
45l 9 million	0.57	136.34	202.70
60l 9 million	0.56	151.63	234.49
60l ideal nr	0.65	89.71	127.68
75l 9 million	0.71	46.93	69.17
75l ideal nr	0.70	47.30	69.22
90l 10 million	0.86	29.96	47.15
90l ideal nr	0.86	30.20	47.19
137l ideal nr	0.67	66.16	85.25

Figure 2: Spatial correlation (r), MBE, and RMSE between ERA5 and the diagnosed precipitation (P), evaporation (E), and surface sensible heat flux (H) fields obtained with FLEXPART v10.4 and HAMSTER v1 for different FLEXPART configurations. Level definitions: **45l**: "lowest" 30 levels are taken (137 to 108) and from then on then every other level 15 times (so until 78); **60l**: whole level range is covered: 1/5/9/13/17/21/25/29/33/37/41/45/49/53/57/61/65/69/73/77/81/85/89/93/97/100/102/104/106/107/108/109/110/111/112/113/114/115/116/117/118/119/120/121/122/123/124/125/126/127/128/129/130/131/132/133/134/135/136/137; **75l**: "lowest" 60 levels are taken (137 to 78) and from then on every other level 15 times (so until 48) e.g. 48/50/52/54/.../74/76/78/79/80/.../135/136/137; **90l**: "lowest" 90 levels are taken. Ideal nr is defined as the number of vertical levels x 361 x 720.

Changes: We added the following sentence to Sect. 2.1 (L151–153)

"The number of particles is chosen to ensure adequate sampling of the atmospheric column based on FLEXPART's internal consistency criterion (i.e. ratio between the maximum number of particles in any column and the number of vertical model levels >

1). *The resulting particle density provides sufficient representation of the vertical structure across atmospheric columns while maintaining computational efficiency.*”

3. As this is primarily a data paper, the inclusion of the HAMSTER v2 update requires further motivation. The authors should clarify why this software update is being introduced here rather than in a dedicated technical or software-focused manuscript. Furthermore, if HAMSTER v2 is to be included, a more rigorous and comprehensive evaluation of the tool’s performance is required.

Author response: We thank the reviewer for this comment and agree that the inclusion of HAMSTER v2 requires clearer motivation in the context of a data paper. HAMSTER v2 is not intended as a central contribution of the manuscript, and therefore a comprehensive technical evaluation of the tool would be beyond its scope. Its inclusion is necessary to demonstrate how the Lagrangian trajectory dataset can be used for moisture and heat tracking applications, and to provide users with a reproducible reference workflow. In this sense, HAMSTER v2 should be understood as an illustrative and enabling tool, while the dataset itself remains fully independent and usable with alternative analysis frameworks.

Following the reviewer’s comment, we have decided to move some of the technical details of the HAMSTER v2 updates to a separate technical note on Zenodo (<https://zenodo.org/records/20181215>), as this material is not central to the scope of the data paper.

Changes:

Technical details on HAMSTER v2 updates were moved from the main text to Appendix B, now entitled “*HAMSTER v2 updates and limitations*”. The following sentence was added to the manuscript (L172–173):

“A description of HAMSTER v2 updates relative to earlier versions is provided in Appendix B, and the model code is openly available on Zenodo (Sect. 5).”

In addition, the Zenodo reference was added to the “Data and code availability” section (L417–418): *“... and archived on Zenodo (<https://zenodo.org/records/20181215>, Insua-Costa et al., 2026).”*

Technical Comments

L72: I suggest mentioning cyclones here (e.g., Papritz et al., 2021; Pérez-Alarcón et al., 2023).

Author response: We thank the reviewer for this suggestion.

Changes: We have rephrased the sentence and added the suggested references (Papritz et al., 2021; Pérez-Alarcón et al., 2023) to the list of applications of Lagrangian moisture tracking (L74–78). It now reads:

“...ranging from large-scale circulation features such as monsoons and climate variability to synoptic systems like cyclones and atmospheric rivers, as well as mesoscale phenomena including low-level jets. They are also widely used for attributing hydrometeorological extremes — such as floods, droughts, and heatwaves — to their upwind moisture sources (e.g., Vázquez et al., 2018; Winschall et al., 2014; Papritz et al., 2021; Pérez-Alarcón et al., 2023; Schumacher et al., 2019; Li et al., 2024a).”

L87: Consider also citing Keune et al. (2022) here.

Author response: We thank the reviewer for pointing this out.

Changes: We have added the reference to Keune et al. (2022) at the indicated location (L92).

L245: This statement is currently ambiguous and requires clarification. While HAMSTER applies a bias correction during moisture tracking, the raw Lagrangian trajectories described in this paper have not undergone a bias correction. Please distinguish clearly between the raw data and the post-processed outputs.

Author response: We agree that the original sentence did not clearly distinguish between the raw trajectory dataset and the bias-corrected diagnostics derived during post-processing.

Changes: The sentence has been revised to clearly distinguish between raw trajectories and post-processing (L253–255):

“By enabling the derivation of spatially explicit, bias-corrected E2P climatologies over more than four decades, the dataset, when combined with post-processing frameworks such as HAMSTER, extends previous studies in temporal coverage and internal consistency...”

L274: The claim that these are "...the first global fields that provide a proxy for the influence of sensible heat on temperature (H2T)" may be an overstatement, given that it is presented as a dataset usage example. I recommend either toning down this claim or providing a more rigorous evaluation to support it.

Author response: We agree that the original phrasing may have been too strong given that this is presented as a usage example.

Changes: We have toned down the statement (L283). It now reads:

“Figure 5 presents a global-scale example of fields that provide a proxy for the influence of sensible heat on atmospheric temperature (H2T).”

L330/L341: Could the authors provide further insights into the specific physical mechanisms driving heat transport from North America to the heatwave region in northeastern China?

Author response: We thank the reviewer for this interesting question. While a detailed dynamical analysis of the underlying physical mechanisms is beyond the scope of this study, we think that the observed signal is likely associated with long-range transport of air masses via the mid-latitude westerlies, which can enable the downstream advection of heat anomalies from North America toward East Asia under favourable large-scale circulation conditions.

Changes: Added this to the following sentence (L350–352):

“North America, for example, contributes ~11 % despite its extreme distance from the heatwave box, likely reflecting long-range transport by the prevailing mid-latitude westerly winds.”

Extra references added to manuscript:

Papritz, L., Aemisegger, F., & Wernli, H. (2021). Sources and transport pathways of precipitating waters in cold-season deep North Atlantic cyclones. *Journal of the Atmospheric Sciences*, 78(10), 3349-3368. <https://doi.org/10.1175/JAS-D-21-0105.1>.

Pérez-Alarcón, A., Coll-Hidalgo, P., Fernández-Alvarez, J.C., Trigo, R.M., Nieto, R., Gimeno, L. (2023). Impacts of tropical cyclones on the global water budget. *npj Climate and Atmospheric Science*, 6, 212. <https://doi.org/10.1038/s41612-023-00546-5>

Insua-Costa, D., Deman, V. M. H., and Miralles, D. G.: Heat And Moisture Tracking fromEwoRk version 2.0 (HAMSTER v2) (2.0.0), Zenodo, <https://doi.org/10.5281/zenodo.20181215>, 2026.